Acta Crystallographica Section D
Biological Crystallography
ISSN 0907-4449

The structures of α_{2u}-globulin and its complex with a hyaline droplet inducer

Barnali N. Chaudhuri,[a] Gerard J. Kleywegt,[a] Joakim Björkman,[b] Lois D. Lehman-McKeeman,[c] Joel D. Oliver[c] and T. Alwyn Jones[a]*

[a]Department of Cell and Molecular Biology, Uppsala University, Biomedical Centre, Box 590, SE-751 24 Uppsala, Sweden, [b]Department of Molecular Biology, Swedish University of Agricultural Sciences, Biomedical Centre, Box 590, SE-751 24 Uppsala, Sweden, and [c]The Procter and Gamble Company, Miami Valley Laboratories, PO Box 398707, Cincinnati, Ohio 45239-8707, USA

Correspondence e-mail: alwyn@xray.bmc.uu.se

Received 6 October 1998
Accepted 5 December 1998

PDB References:
α_{2u}-globulin, 2a2u;
α_{2u}-globulin–*d*-limonene epoxide complex, 2a2g.

α_{2u}-Globulin (A2U) is the major urinary protein excreted by adult male rats. The structure of a monoclinic crystal form of A2U was reported in 1992 [Böcskei *et al.* (1992). *Nature (London)*, **360**, 186–188]. The structures of an orthorhombic crystal form of A2U at 2.5 Å resolution (refined to an *R* factor of 0.248; R_{free} = 0.264) and of a complex between A2U and *d*-limonene 1,2-epoxide (DLO) at 2.9 Å resolution (*R* factor = 0.248; R_{free} = 0.260) are presented here. DLO is one of a diverse group of chemicals which cause a male rat-specific renal carcinogenesis called hyaline-droplet nephropathy. The rate-determining step in the development of this disorder is the binding of the toxin to A2U. Comparison of the cavities in A2U and in the corresponding mouse urinary protein (MUP) reveal that the former is tailor-made for small oval hydrophobic ligands such as DLO. The cavity in MUP is more shallow and elongated and cannot easily accommodate such ligands.

1. Introduction

α_{2u}-Globulin (A2U) is the major urinary protein excreted by adult male rats, making up 30–50% of the excreted protein in urine (Roy *et al.*, 1966). Although its exact physiological role is not known, it probably functions as a pheromone-binding protein in the urine of mature male rats (Cowley, 1978). The sex and age specificity and strict androgenic control of its synthesis supports this hypothesis, although the physiological ligand of A2U remains unknown.

A2U belongs to a large superfamily of proteins called the lipid-binding protein (LBP) superfamily (Banaszak *et al.*, 1994). Sequence similarities within the superfamily are weak and limited to a cluster of interactions which are close together in three dimensions (Jones *et al.*, 1988). The superfamily can be divided into two subfamilies, both of which contain an orthogonal β-barrel which encapsulates small hydrophobic or amphipathic ligands. The extracellular LBP (eLBP) family (Banaszak *et al.*, 1994) contains proteins which typically consist of 160–200 amino acids and fold into an eight-stranded antiparallel β-barrel with N- and C-terminal extensions, as first seen in the structure of plasma retinol-binding protein (RBP; Newcomer *et al.*, 1984; Cowan *et al.*, 1990). Within this family, sequence similarities tend to be low (Pervaiz & Brew, 1985; Flower *et al.*, 1993; Flower, 1996; Toh *et al.*, 1996). Crystal structures have been determined for several members of the family, namely RBP (Newcomer *et al.*, 1984; Cowan *et al.*, 1990; Zanotti *et al.*, 1993, 1994), β-lactoglobulin (BLG; Papiz *et al.*, 1986; Monaco *et al.*, 1987; Brownlow *et al.*, 1997), bilin-binding protein (BBP; Holden *et al.*, 1987; Huber *et al.*, 1987),

mouse major urinary protein (MUP; Böcskei *et al.*, 1992), A2U (Böcskei *et al.*, 1992), epididymal retinoic acid binding protein (Newcomer, 1993) and odorant-binding protein (OBP; Tegoni *et al.*, 1996; Bianchet *et al.*, 1996).

Research has shown that a diverse group of chemical agents, which are small and mainly hydrophobic in nature, can induce a type of renal carcinogenesis, named hyaline-droplet nephropathy, which is specific for male rats (Borghoff *et al.*, 1990; Lehman-McKeeman, 1993). The hallmark of this acute toxicity is the accumulation of hyaline droplets within the epithelial cells of the renal proximal convoluted tubule. Compounds that induce this toxicity include *d*-limonene (DL, *p*-mentha-1,8-diene), decalin, 1,3,5-trinitrobenzene, 2,2,4-trimethylpentanol, gabapectin (an anti-epileptic/anti-convulsant therapeutic agent), 1,8-cineole and *p*-dichlorobenzene (Stonard *et al.*, 1986; Bomhard *et al.*, 1990; Ridder *et al.*, 1990; Borghoff *et al.*, 1991; Takahashi *et al.*, 1993; Kristiansen & Madsen, 1995; Kim *et al.*, 1997). Interestingly, a number of hyaline-droplet inducers have been tested on female rats, male and female mice, guinea pigs, dogs and monkeys, and have been shown not to induce any accumulation of hyaline droplets (Lehman-McKeeman & Caudill, 1992*a*,*b*). The rate-limiting step of the toxicity has been shown to be the binding of A2U to these compounds (Dietrich & Swenberg, 1991).

A minor oxidation product of DL in rat liver, the *cis* form of *d*-limonene 1,2-epoxide (DLO; Fig. 1*a*), has been identified as the main hyaline-droplet inducer in rat kidneys (Lehman-McKeeman *et al.*, 1989). It binds strongly but reversibly to A2U, with a K_d of the order of 10^{-7} *M*. DLO accounts for more than 80% of the binding, whereas DL itself and its other metabolites account for 13 and 5% of the binding, respectively. DLO has been shown not to bind to any other protein in the eLBP family, including MUP, despite the high structural similarity between A2U and MUP (Lehman-McKeeman & Caudill, 1992*a*,*b*). However, the endogenous ligand of MUP, 2-*sec*-butyl-4,5-dihydrothiazole (DHT; Fig. 1*b*) is a competitive inhibitor of DLO, binding to A2U with high affinity, and is also a hyaline-droplet inducer in rats (Lehman-McKeeman *et al.*, 1998).

The exclusive selectivity of these hydrophobic compounds to a particular member of a family of closely related proteins with highly similar structures is noteworthy, since hydrophobic binding is nonspecific in nature. The purpose of the present investigation was to determine the structure of A2U with and without bound DLO and to investigate the nature of the ligand-binding pocket. The structures of A2U with and without DLO are compared with the structure of MUP. Since MUP and A2U have the same fold and a similar hydrophobic pocket, the structural basis for the specificity of DLO for the rat protein is expected to lie in the detailed conformation of the residues lining the surface of the cavity.

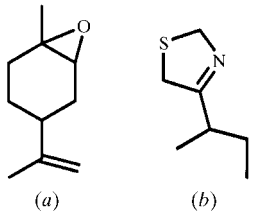

Figure 1
Chemical structures of (*a*) *d*-limonene 1,2-epoxide (DLO) and (*b*) 2-*sec*-butyl-4,5-dihydrothiazole (DHT). DLO can exist in *cis* and *trans* conformations (these are geometrical isomers; the names *cis* and *trans* refer to the orientation of the epoxide group with respect to the isopropylene group).

2. Materials and methods

2.1. Protein purification, crystallization and data collection

The A2U used in this work was purified from male rat urine as described previously (Lehman-McKeeman *et al.*, 1990) with minor modifications. Briefly, urine was collected over dry ice and kept frozen at 193 K pending purification. Total urinary protein was isolated by gel-filtration chromatography (PD-10 columns, Pharmacia, Piscataway, NJ) and then concentrated with an evaporator/concentrator. A2U was isolated from the concentrated total protein sample by anion-exchange HPLC. Chromatography was performed on a preparative Synchropak AX-300 column (25 × 4.6 cm; Rainin Instruments, Woburn, MA). Approximately 5 mg of the total urinary protein was injected onto the column, after which proteins were eluted with a linear gradient of Tris–HCl mobile phase (solvent *A*, 10 m*M* Tris–HCl pH 7.4 at 298 K; solvent *B*, 10 m*M* Tris–HCl/0.5 *M* NaCl, pH 7.4) from 0–100% solvent *B* in 25 min at a flow rate of 3 ml min^{-1} and detected at 280 nm. The peak representing A2U was collected and desalted by three successive applications to Sephadex G-25 columns, as described previously. The purified desalted protein was then concentrated to approximately 10 mg ml^{-1} for use in crystallization trials. The concentrated protein solution was stored at 193 K when not in use. MALDI mass spectrometry revealed a single component (MH^+ = 18731.8 Da, corresponding to the molecular weight of A2U). The entire amino-acid sequence of the protein was confirmed by Edman sequencing following proteolytic degradation.

For studies involving DLO bound to A2U, the purified protein used as above was mixed with an excess of the epoxide (a mixture of the *cis* and *trans* isomers; from Aldrich Chemical Co., Milwaukee, WI) and allowed to incubate for 1 h at 277 K. An equilibrium saturation-binding experiment showed previously that under the above-mentioned conditions, the molar ratio of ligand to protein is 0.95 (Lehman-McKeeman & Caudill, 1992*b*). The conjugated protein was re-isolated by Sephadex G-25 chromatography, desalted and again concentrated to approximately 10 mg ml^{-1} for use in crystallization trials.

After shipment to Sweden, the protein was checked by SDS–PAGE to ensure that the sample had not degenerated during transportation. Crystals of the uncomplexed protein were obtained using the hanging-drop vapour-diffusion method (McPherson, 1982). 2.5 µl of protein solution (10 mg ml^{-1}) was added to an equal volume of reservoir

Table 1
Crystal data and data-processing, scaling and merging statistics.

Values in parentheses are for the highest resolution shell.

	A2U	A2U–DLO
Space group	$P2_12_12_1$	$P2_12_12_1$
Unit-cell dimensions (Å)	62.3, 106.8, 114.2	62.8, 98.0, 123.4
Number of crystals	1	2
Temperature (K)	290	277
Asymmetric unit contents	4 molecules	4 molecules
V_m† (Å^3 Da^{-1})	2.5	2.5
Range of Bragg spacings (Å)	48–2.5 (2.7–2.5)	49–2.9 (2.98–2.9)
Number of observed reflections	78794	49636
Number of unique reflections	25797	15350
Completeness (%)	95.1 (94.6)	88.0 (91.3)
Average multiplicity	3.1 (1.9)	3.2 (3.1)
$R_{\rm merge}$‡	0.082 (0.26)	0.102 (0.35)
$\langle I/\sigma(I)\rangle$	13.5 (1.9)	11.3 (3.6)

† As defined by Matthews (1968). ‡ $R_{\rm merge} = \sum_h \sum_i |I_{h,i} - \langle I_h\rangle| / \sum_h \sum_i |I_{h,i}|$.

solution containing 15% PEG 4000, 300 m*M* $(NH_4)_2SO_4$ or 500 m*M* NaCl, and 50 m*M* Na_3PO_4 (pH range 4.1–4.7). Crystals grew within a week to a final size of approximately 0.6 × 0.3 × 0.2 mm. All data were collected on a Hamlin area-detector (Hamlin *et al.*, 1981) and processed with the accompanying software package (Howard *et al.*, 1985). Three different crystal forms were obtained, all in space group $P2_12_12_1$, but with different unit-cell parameters: form I, $a = 62.3$, $b = 106.8$, $c = 114.2$ Å; form II, $a = 61.3$, $b = 99.9$, $c = 123.4$ Å and form III, $a = 61.0$, $b = 99.4$, $c = 105.9$ Å. Although complete data sets were collected for all three crystal forms, form I is the one used and described here (Table 1). None of the three crystal forms is isomorphous to the one reported previously (Böcskei *et al.*, 1992).

Crystals of the A2U–DLO complex were grown from the concentrated (10 mg ml^{-1}) complex using the sitting-drop vapour-diffusion method at 277 K. The reservoir solution consisted of 10–20% PEG 4000, 0.1 *M* sodium acetate buffer (pH 4.0) and 0.175 m*M* $(NH_4)_2SO_4$. Crystals of form II appeared after a period of 4–5 weeks. The largest crystals had dimensions of 0.3 × 0.2 × 0.2 mm. Since these crystals did not survive trips to the synchrotron, all data for the complex were collected using an in-house R-AXIS IIC image-plate detector mounted on a Rigaku rotating-anode generator. The data sets were processed with *DENZO* (Otwinowski & Minor, 1997) and scaled and merged with *SCALA* (Collaborative Computational Project, Number 4, 1994) (Table 1).

2.2. Structure solution and refinement

Early attempts to solve the structure of A2U with molecular-replacement techniques (Rossmann & Blow, 1962; Rossmann, 1972) using the structure of RBP (Newcomer *et al.*, 1984; Cowan *et al.*, 1990; PDB code 1RBP) as a search model failed, probably owing to the fact that there are four A2U molecules present in the asymmetric unit. Co-crystallization with mercury acetate resulted in a useful heavy-atom derivative with the same unit-cell parameters as wild-type crystal form I. Using difference Patterson and cross-Fourier maps, four heavy-atom positions were identified, presumably one for each monomer. However, the SIR maps obtained using the single derivative proved to be uninterpretable. Attempts to obtain other derivatives were not successful.

In 1992, the structure of a monoclinic form of A2U was solved and partially refined by Böcskei and co-workers in Leeds at a resolution of 2.8 Å (Böcskei *et al.*, 1992). Dr S. E. V. Phillips kindly provided us with the coordinates of the complete tetramer model (this model of A2U is not deposited in the PDB). Our structure was subsequently easily solved with molecular-replacement techniques using the program *X-PLOR* (Brünger, 1990*a*). The search model consisted of the tetramer, with all temperature factors reset to 20 Å^2. The rotation function (using data between 15.0 and 4.0 Å) gave two solutions which were ∼1.5σ better than the next solution. The 21 best solutions were subjected to Patterson correlation (PC) refinement (Brünger, 1990*b*), consisting of 50 cycles of rigid-body refinement with the four monomers as separate rigid bodies. After this, solutions 21, 2 and 1 had PC values about twice as high as the next best solution (0.177, 0.174 and 0.167, respectively; next best was 0.085). All three solutions were related by rotations of ∼180°. Since the search model was the complete tetramer, one would expect to find four equivalent high-scoring solutions, all related by 180° rotations. Apparently, the fourth solution was not among the 21 best solutions of the rotation function (note that rotation-function solution 21 became the highest scoring solution after PC refinement). The solution with the highest PC value was used for the translation function. The highest peak by far had a translation function value ∼10σ higher than the second-best solution (0.617 *versus* 0.401, σ = 0. 021). This model had an *R* factor of 0.386 using data between 8.0 and 3.0 Å, which dropped to 0.367 after 50 cycles of rigid-body refinement.

The structure of the A2U–DLO complex was also solved with the molecular-replacement method, using the program *AMoRe* (Navaza, 1994) with the refined model of the uncomplexed protein as the search model. Data in the resolution range 10.0–3.5 Å were used for the rotation- and translation-function calculations. After the initial rotational search, the first molecule was located by means of a centred-overlap translational search, yielding an *R* factor of 0.444 and a correlation coefficient of 0.286. The remaining three molecules were found using phased translation functions (Navaza & Saludjian, 1997). After rigid-body refinement, the *R* factor for the complete tetramer was 0.239 and the correlation coefficient was 0.781 (10.0–3.5 Å).

In view of the limited resolution, both models were refined conservatively (Kleywegt & Jones, 1995, 1997*a*). In order to prevent overfitting, the fourfold NCS was constrained, temperature factors were modelled by group and the progress of refinement was carefully monitored using the free *R* value (Brünger, 1992; Kleywegt & Brünger, 1996). Even for the 2.5 Å A2U structure, replacing the NCS constraints by restraints did not improve the model as judged by the behaviour of the free *R* value (Kleywegt & Brünger, 1996). Most refinement cycles involved Powell minimization, high-temperature simulated annealing (Brünger *et al.*, 1987, 1990)

and grouped temperature-factor optimization. In between refinement cycles, models were subjected to critical quality analyses and then rebuilt in *O* (Jones *et al.*, 1991) in NCS-averaged electron-density maps. All refinement was carried out using the Engh and Huber force field (Engh & Huber, 1991) for the protein.

2.3. Quality of the final models

The final model of both native A2U and the A2U–DLO complex includes the first 158 amino-acid residues (four C-terminal residues, Gln–Ala–Arg–Gly, are not visible in any of the maps). 17 water molecules were located in the A2U structure, whereas no water was modelled for the A2U–DLO complex. The sequence of A2U contains one potential N-glycosylation site (at Asn35), but there is no evidence for glycosylation in any of the electron-density maps. This is in agreement with the finding that unprocessed A2U is glycosylated, but that the sugar is removed prior to secretion of the protein from the liver (Chatterjee *et al.*, 1982). The density for the protein is generally good, especially in the fourfold NCS-averaged maps, with the exception of several residues near the N-terminus (5—9), some residues in the range 60–65 and a few more isolated residues in both structures. Although the uncomplexed protein was expected to be devoid of any ligand, the electron-density maps show clear density for an indigenous ligand (Fig. 2*a*), just as was observed in the monoclinic crystal form (Böcskei *et al.*, 1992). The nature of this ligand is unknown, and no attempt has been made to model this density. Surprisingly, when A2U was subjected to thermal desorption with subsequent GC/MS analysis, no ligand could be detected (Lehman-McKeeman *et al.*, 1998).

DLO can occur in different isomers (*cis*/*trans*) and conformations (ring puckering). Since no crystal structure of this compound is available, plausible structures were determined using graphical, molecular-mechanics, semi-empirical and *ab initio* quantum-chemical calculations (B. Laidig & M. Schmidt, University of Florida, personal communication). These calculations yielded six *cis* and six *trans* conformations. In the averaged map of the complex, there is clear density in the cavity for DLO (Fig. 2*b*). However, owing to the limited resolution of our study and the possibility of multiple conformations, we could not model the ligand unambiguously in the density. Therefore, the ligand DLO has not been included in the refinement. The *R* factors for the final models were (with constrained fourfold NCS and group temperature-factor constraints) 0.248 ($R_{\rm free}$, 0.264) and 0.248 ($R_{\rm free}$, 0.260) for A2U and the A2U–DLO complex, respectively. From an $R_{\rm free}$-based Luzzati plot (Luzzati, 1952; Kleywegt & Brünger, 1996), we estimate the average coordinate error to be ∼0.4 and ∼0.45 Å for A2U and the A2U–DLO complex, respectively. Although seven residues for the uncomplexed form and eight residues for the complexed form are outliers in the Ramachandran plot (Ramakrishnan & Ramachandran, 1965; Kleywegt & Jones, 1996*a*), only one (Tyr97) lies far removed from any core areas in the Ramachandran plot of both models. However, this residue has excellent density, and it is also an outlier in several related structures, such as RBP (Tyr111), and is a feature of the family (Cowan *et al.*, 1990). Ramachandran plots for the final models are shown in Fig. 3(*a*) (A2U) and Fig. 3(*b*) (A2U–DLO complex). Details of the refinement and the final models are given in Table 2.

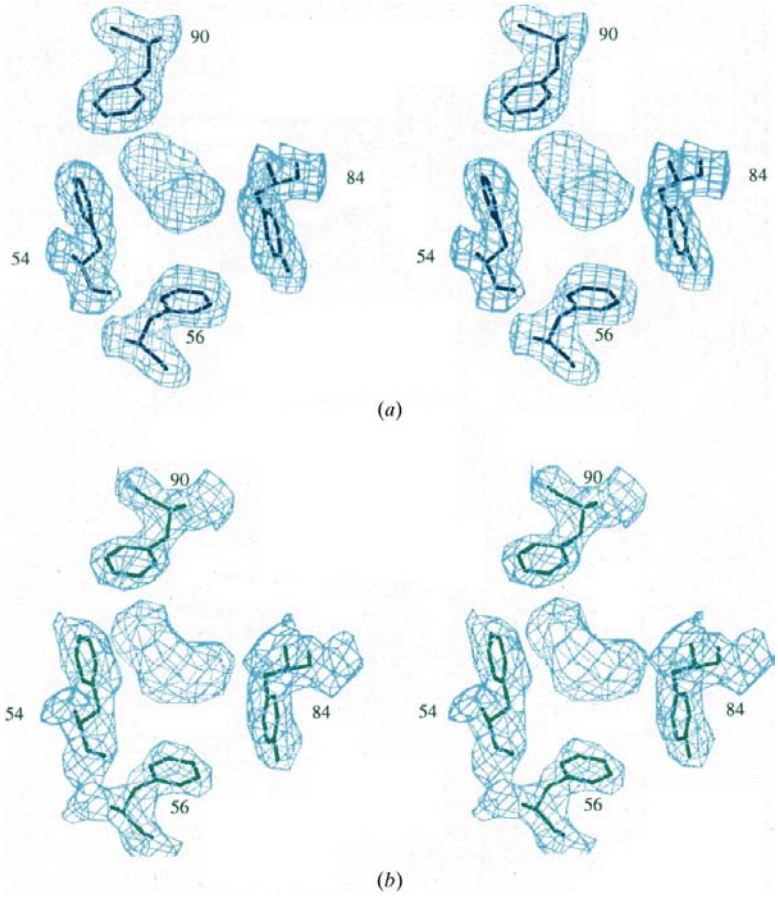

Figure 2
Representative averaged density for (*a*) A2U and (*b*) the A2U–DLO complex is shown in similar orientations. Averaged density for the unknown ligand in A2U and for DLO in the A2U–DLO complex is also shown. This figure, and Figs. 4, 5, 6 and 7, were prepared using *O* and *OPLOT* (M. Kjeldgaard, unpublished program).

2.4. Software used

All model-building, rebuilding, modelling, structure-alignment and graphics operations were carried out with the crystallographic modelling program *O* (Jones *et al.*, 1991). Molecular-replacement calculations for A2U, as well as all structure refinement, were carried out with *X-PLOR* (Brünger, 1990*a*). The structure of the A2U–DLO complex was solved with the program *AMoRe* (Navaza, 1994; Navaza & Saludjian, 1997) and refined with the programs *X-PLOR* and *CNS* (Brünger *et al.*, 1998). Electron-density averaging

Table 2
Refinement and final model statistics.

Values were calculated with *O* (Jones *et al.*, 1991), *X-PLOR* (Brünger, 1990*a*), *CNS* (Brünger *et al.*, 1998), *PROCHECK* (Laskowski *et al.*, 1993), *WHAT IF* (Vriend & Sander, 1993) and *MOLEMAN*2 (G. J. Kleywegt, unpublished program).

	A2U	A2U–DLO
Resolution range (Å)	8.0–2.5	10.0–2.9
Number of reflections ($F > 0$)	22189	13705
Final R factor†	0.248	0.248
Last recorded value of R_{free}†	0.264	0.260
NCS model	Constrained	Constrained
B-factor model	Grouped (mc/sc)	Grouped (mc/sc)
Number of protein atoms ($Z > 1$)	1288	1288
Number of solvent atoms ($Z > 1$)	17	0
Average temperature factors (Å^2)		
Main-chain atoms	32.9	37.9
Side-chain atoms	51.7	46.5
Water O atoms	42.5	n/a
R.m.s. deviations from ideal geometry‡		
Bond lengths (Å)	0.009	0.005
Bond angles (°)	1.3	1.4
Residue-based quality descriptors		
Ramachandran plot outliers §	7	8
Unusual peptide orientations¶	1	4
Non-rotamer side-chain conformations††	6	3
Weak averaged density‡‡	7	19§§
Overall structural quality		
Overall DACA score¶¶	+0.08	−0.28
Overall G factor†††	+0.25	+0.30

† $R = \sum ||F_o| - |F_c|| / \sum |F_o|$; R_{free} is the same, but calculated for a subset of reflections which are not used in the refinement; F_o and F_c are the observed and calculated structure factors, respectively. ‡ Calculated with *X-PLOR* using the Engh & Huber (1991) force field. § Calculated with *MOLEMAN*2 using the definition of Kleywegt & Jones (1996*a*). ¶ Calculated with *O* (Pep_flip) using a cutoff of 2.5 Å. †† Calculated with *O* (RSC_fit) using a cutoff of 1.5 Å. ‡‡ Calculated with *O* and *CNS*; defined as the number of residues for which the real-space fit (correlation coefficient) to the final averaged map is less than 0.70. ¶¶ Calculated with *WHAT IF*. §§ The nine N-terminal residues are not visible in the averaged or unaveraged maps. †††Calculated with *PROCHECK*.

was carried out with the *RAVE* software package (Jones, 1992; Kleywegt & Jones, 1994*a*). All map calculations were performed with various programs in the *CCP*4 package (Collaborative Computational Project, Number 4, 1994) and *CNS*. The quality of intermediate and final models was assessed with *O*, *X-PLOR*, *PROCHECK* (Laskowski *et al.*, 1993), *OOPS* (Kleywegt & Jones, 1996*b*) and *WHAT IF* (Vriend & Sander, 1993). Cavities were investigated with *VOIDOO* (Kleywegt & Jones, 1994*b*) and structural similarities between A2U and other proteins were analysed with *LSQMAN* (Kleywegt, 1996), *DEJAVU* (Kleywegt & Jones, 1997*b*), *SPASM* (Kleywegt & Jones, 1998; Kleywegt, 1999) and *O*. Accessible surface areas were calculated with the program *ASA* (Lee & Richards, 1971).

3. Results and discussion

3.1. Overall structure

In both the structures reported here, the A2U monomer has the folding topology described previously (Böcskei *et al.*, 1992). This fold consists of an eight-stranded β-barrel made up of two antiparallel orthogonal β-sheets, with both N- and C-terminal extensions (Fig. 4). The larger extension at the C-terminus of the barrel consists of an α-helix, which packs onto one face of the barrel, followed by a loop which brings the C-terminal part of the protein back to the other face of the barrel. In both A2U and MUP (Böcskei *et al.*, 1992), the N-terminal extension forms a short β-strand not present in RBP (Cowan *et al.*, 1990).

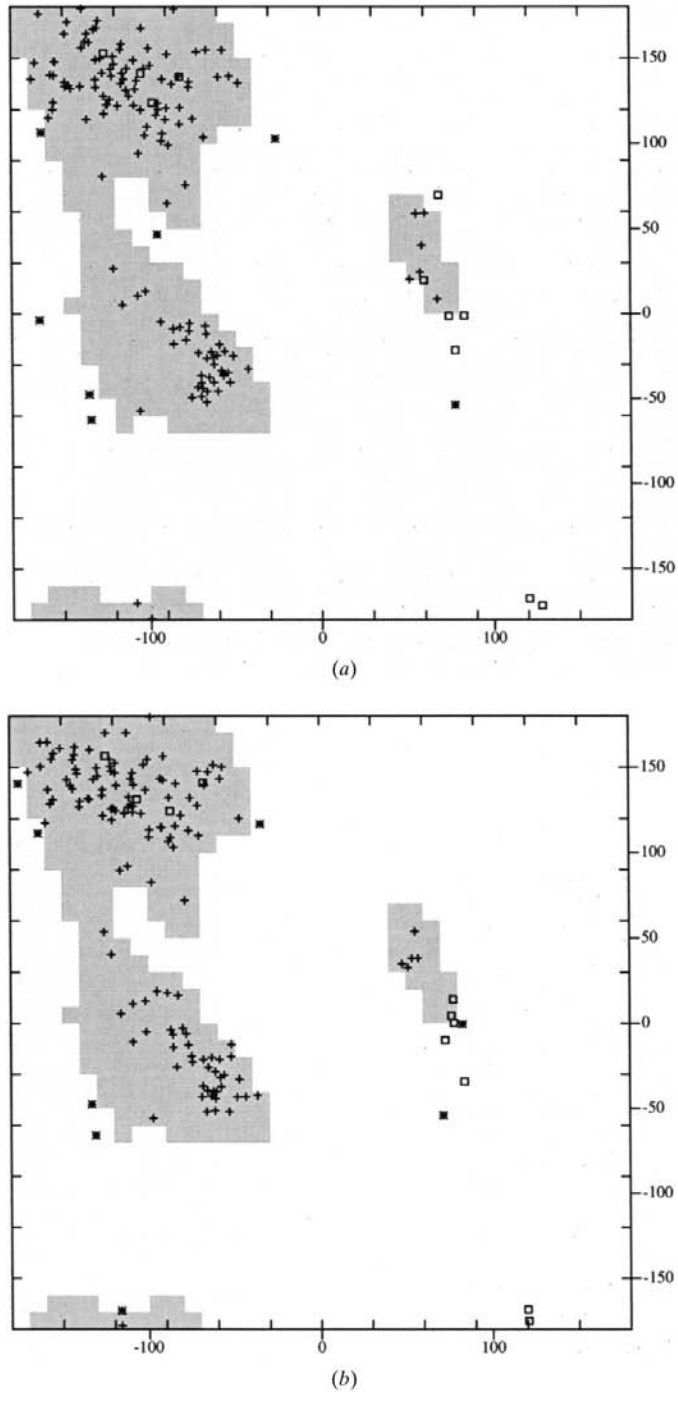

Figure 3
Ramachandran plots for the final monomer models of (*a*) A2U and (*b*) A2U–DLO.

Table 3
Comparison of the A2U structure with A2U–DLO and other eLBP family members.

The structural alignments were carried out with *LSQMAN* (Kleywegt, 1996) using a cutoff distance of 3.6 Å.

Protein	PDB code†	N_r‡	N_m§	N_c¶	R.m.s.d.†† (Å)	Reference
A2U–DLO	—	158	158	158	0.27	This work
MUP	1MUP (A)	157	151	98	0.88	Böcskei *et al.* (1992)
OBP	1OBP (A)	158	108	30	1.20	Bianchet *et al.* (1996)
OBP	1OBP (A+B)	(313)	129	37	1.26	Bianchet *et al.* (1996)
eRABP	1EPA (A)	160	111	24	1.55	Newcomer (1993)
BLG	1BEB (A)	156	131	34	1.56	Brownlow *et al.* (1997)
BBP	1BBP (A)	173	89	16	1.87	Huber *et al.* (1987)
RBP	1RBP (A)	174	107	17	1.88	Newcomer *et al.* (1984)

† The name of the chain(s) used in the alignment is shown in parentheses. ‡ The number of residues in the aligned chain(s). § The number of structurally equivalent residues. ¶ The number of structurally equivalent residues which are conserved in the sequence. †† R.m.s.d. of the structurally equivalent residues.

The structure contains one disulfide bridge (Cys64 and Cys157) as well as one free cysteine (138), surrounded by hydrophobic residues. The disulfide bridge lies near the surface of the protein and anchors the C-terminal part of the protein to the core of the barrel.

Four A2U monomers form a tetramer with 222 symmetry in the asymmetric unit of the cell. All molecules are related by rotations of ~180°, with screw components along the rotation axes being of the order of 0.1 Å or less.

During the rebuilding of the A2U model, the tracing of the N-terminus, the turn 59–64 and the C-terminus was slightly revised compared to the model of the monoclinic form. The r.m.s.d.s on C^{α} atoms between the final model of the orthorhombic form and the four partially refined molecules of the monoclinic crystal form (Böcskei *et al.*, 1992) vary from 0.7 to 1.3 Å for 157 common residues. The refined models of uncomplexed and complexed A2U are essentially identical (r.m.s.d. 0.3 Å on C^{α} atoms).

3.2. The ligand-binding cavity

All the residues that line the extremely hydrophobic inner surface of the β-barrel cavity have well defined density in the averaged maps and have the same side-chain conformations in both models. In what was supposed to be a crystal of A2U devoid of any ligand, clear density for an unknown ligand is nevertheless observed (Fig. 2*a*); unaccounted density was also observed in the monoclinic crystal form (Böcskei *et al.*, 1992). The density is equally clear in averaged and unaveraged maps, indicating that the ligand must have appreciable occupancy. The nature of the cavity makes it likely that the ligand is hydrophobic, but the limited resolution does not allow its chemical structure to be determined.

Owing to the limited resolution, we could not model the ligand DLO (Fig. 1*a*) into its density unambiguously. Both the *cis* and *trans* form of DLO can be fitted to the density without introducing unfavourable contacts with the protein. The open diol form, which is a metabolite of DL in rats and might be present considering the low experimental pH and the reversible nature of binding, would also fit the density, although it accounts for a very small portion of binding *in vivo*. Hence, the density we observe could be a mixture of different conformations of different compounds.

The averaged $2F_o - F_c$ electron density of DLO in the complex indicates a very good shape complementarity. There are only two polar protein groups which can possibly interact with the epoxide moiety of DLO. The hydroxyl group of Tyr120 is pointing straight towards the ligand density and is discussed later. Another candidate is the S atom of Met38. However, since it can only function as a weak hydrogen-bond acceptor, it could only interact with the open diol form of the ligand, which is physiologically less relevant.

3.3. A comparison of the ligand-binding cavity in A2U and MUP

Compared with the other members of the family whose crystal structures are known (Table 3), the structure of A2U is most similar to that of MUP (Fig. 4). If the domain swapping which occurs in the OBP dimer is ignored then OBP has the next most similar structure.

Table 4 contains a list of residues which line the cavity of A2U and MUP and Fig. 5 shows a superposition of both cavities. The cavities share a number of similar features. They are both closed off to the solvent and have a similar volume [84 $Å^3$ for A2U and 76 $Å^3$ for MUP, calculated using *VOIDOO* (Kleywegt & Jones, 1994*b*), using a 1.4 Å probe radius]. Both pockets are extremely hydrophobic, with only a handful of polar atoms in the surface (Met38 S^{δ} and O, Asn88 $O^{\delta1}$ and $N^{\delta2}$ and Tyr120 O^{η} for A2U; Phe42 O, Leu44 N and O, Met73 S^{δ}, Asn92 $O^{\delta1}$ and $N^{\delta2}$, Ala109 N, Leu120 O and Tyr124 O^{η} for MUP).

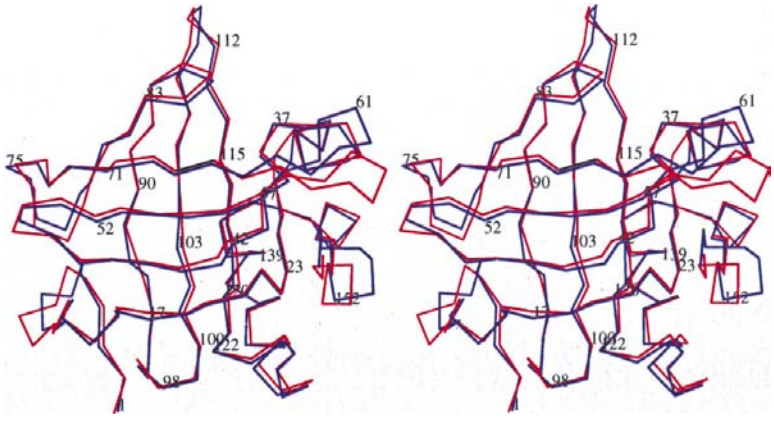

Figure 4
C^{α} traces of superimposed A2U (blue) and MUP (red).

Table 4
Accessible surface area (ASA) of the residues that line the ligand-binding cavity in A2U and MUP.

Structurally equivalent residues are shown on the same line. A dash indicates that the structurally equivalent residue is not part of the cavity surface in one of the proteins.

A2U	ASA (Å^2)	MUP	ASA (Å^2)
Met38	7	Phe42	8
Val40	13	Leu44	17
Met42	10	Leu46	11
—		Ile49	6
Phe54	17	Leu58	14
Phe56	7	Phe60	19
Leu69	44	Met73	21
Val82	12	Val86	15
Tyr84	42	Tyr88	43
Phe90	10	Phe94	22
—		Ile96	4
—		Leu105	5
Phe103	7	Ala107	16
Leu105	22	Leu109	25
Leu116	8	Leu120	13
Val118	5	—	
Tyr120	14	Tyr124	22

There are, nevertheless, some subtle differences such that the overlap between the two cavities is only 40 Å^3, *i.e* only about half of each individual cavity volume. Whereas the cavity in A2U is roughly spherical in shape, the MUP cavity is more elongated and shallow. Roughly half of all the cavity-lining residues in A2U and MUP are identical (Table 4). The remaining residues, however, ensure that the shapes of the cavities are different.

In A2U, Phe54 and Phe103 together with Phe90 inside the cavity are oriented in a pseudo-threefold symmetric arrangement (Fig. 5), forming a very hydrophobic concave wall which can accommodate a hydrophobic ligand with a complementary convex surface. This part of the cavity may house the more hydrophobic side of DLO. In MUP, two of the phenylalanines are replaced by Leu58 and Ala107, elongating the cavity in the region surrounded by Leu19, Leu56, Ile49, Leu58, Ile96, Leu105 and Ala107 (MUP numbering).

Fig. 6 shows a cross section of contiguous cavity-lining residues in A2U and MUP. Two of them are different in sequence and the arrangement of side chains is slightly different. The orientation of the conserved Tyr120 aromatic ring is slightly different in A2U and MUP. In A2U, Tyr120 is wedged in between a valine and a methionine residue, whereas in MUP this residue is between a glycine and a leucine. While the main-chain conformation is similar in both structures, the tyrosine ring is tilted towards Met42 in A2U to accommodate the more bulky valine side chain and the hydroxyl group points towards the ligand density. This tyrosine hydroxyl group in MUP forms a hydrogen bond with the ligand (DHT) *via* a water molecule (Böcskei *et al.*, 1992). The conserved residues Phe56 and Leu67 assume different conformations to accommodate Met42 in A2U. The different orientation of the ring of Phe56 seems critical, since it makes the cavity wall narrower in MUP.

The cavity inside the closely related OBP (Bianchet *et al.*, 1996; Table 3) is also closed off completely, hydrophobic in nature and comparable in size with that of A2U and MUP (90 Å^3). The OBP cavity is elongated as in MUP, but is more curved. On the other hand, the cavities inside RBP (Newcomer *et al.*, 1984) and BBP (Huber *et al.*, 1987) are both connected to bulk solvent. They are much larger and less hydrophobic than the cavities in A2U and MUP. Both cavities are somewhat extended and have only a very small overlap with the cavity in A2U (15 Å^3 for BBP and 18 Å^3 for RBP).

4. Conclusions

4.1. Structural determinants of ligand-binding affinity

The model of the A2U–DLO complex reveals some salient features of the strong complex formation. The key to the strong binding lies in the shape of the cavity, which is complementary to the shape of the ligand. The cavity shape is appropriate to accommodate a small, mainly hydrophobic oval-shaped ligand such as DLO. About one-third of the cavity surface is made up of five aromatic π-electron planes (calculated using the sum of the accessible surface area for the six aromatic ring atoms). Three of them (Phe54, Phe90 and Phe103) form a concave wall on one side and two others (Phe56 and Tyr84) form a part of the roof of the cavity (Fig. 5). In the model of DLO that fits the density best, the isopropylene moiety is accommodated close to the aromatic concave

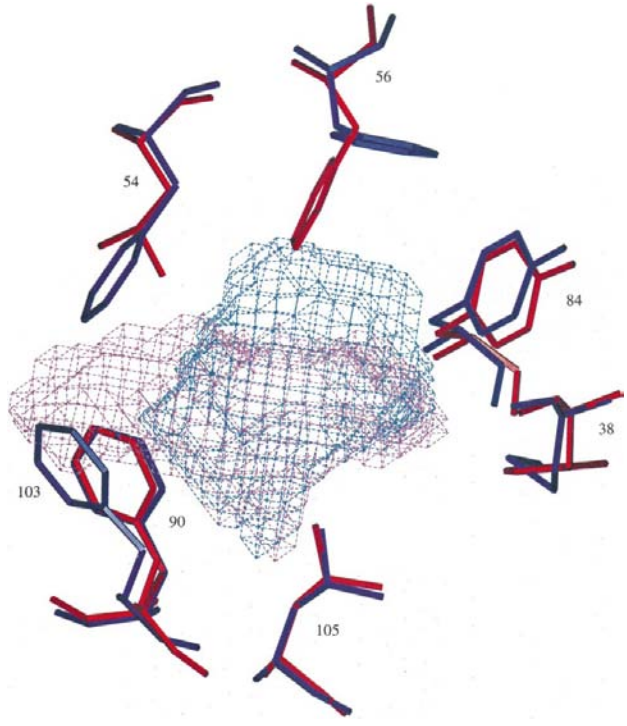

Figure 5
Illustration of the shape of the superimposed ligand-binding cavities of A2U (blue) and MUP (red), with a few surrounding residues. Note the different orientation of Phe56 in the two proteins and its effect on the cavity shape.

surface (Fig. 7). Tyr120 is oriented sideways and its aromatic ring plane does not contribute directly to the ligand-binding surface. Stacking between the aromatic π-cloud and aliphatic/alicyclic H atoms is a favoured mode of interaction for biological macromolecules. Hyaline-droplet inducers are generally small hydrocarbon compounds which can use these accessible aromatic planes advantageously to stack the non-polar H atoms.

The Tyr120 hydroxyl group in A2U is placed in the midst of a very hydrophobic surrounding with unsatisfied hydrogen-bonding capacity and points towards the DLO density (Fig. 6). It seems likely that the polar moiety of DLO interacts with this hydroxyl group (Fig. 7). Formation of a hydrogen bond (either direct or water-bridged) could be important since DLO binds to A2U more strongly than DL, the latter being devoid of the polar epoxide moiety. The corresponding difference in differential Gibbs energy ($\Delta\Delta G$) at room temperature is about 1.8 kcal mol^{-1} (1 kcal mol^{-1} = 4.184 kJ mol^{-1}), which is of the order of an hydrogen bond (L. D. Lehman-McKeeman, unpublished results). The limited conformational flexibility of DLO in comparison with DL, which arises from the presence of the epoxide group, could also favour a more compact packing resulting in a stronger complex.

The endogenous ligand for MUP, DHT (Fig. 1*b*), has also been shown to bind to A2U (Lehman-McKeeman *et al.*, 1998). The inhibition constants of DL and DHT are similar. A model of DHT can be accommodated in the A2U cavity without any steric clashes.

Differences in only a handful of residues and side-chain conformations result in a quite different cavity shape in A2U compared to MUP. MUP is devoid of the concave aromatic wall formed by three phenyl rings in A2U. Instead, the cavity is narrow and extended in this region, being surrounded by hydrophobic residues. A different conformation of Phe56 in MUP makes the cavity wall shallow (Fig. 5). This phenyl ring cannot assume any other conformation because of the steric crowding created by the surrounding residues, which are larger than their counterparts in A2U. This renders the MUP cavity unfit for binding the oval-shaped DLO, whereas the cavity in A2U is more or less 'tailor-made' for this ligand. In our best-fitting model (Figs. 6 and 7), the orientation of DLO is such that it is capable of interacting with the Tyr120 hydroxyl group while simultaneously interacting extensively with the hydrophobic surrounding. 13 out of the 16 cavity-lining residues are almost completely buried upon complexation.

These observations suggest that the steric volume of the ligand might be the principal determinant of its binding affinity. It is fascinating to observe how two proteins with such a high degree of structural and sequence similarity (63% identity) can achieve binding specificity by subtle modulation of the cavity shape.

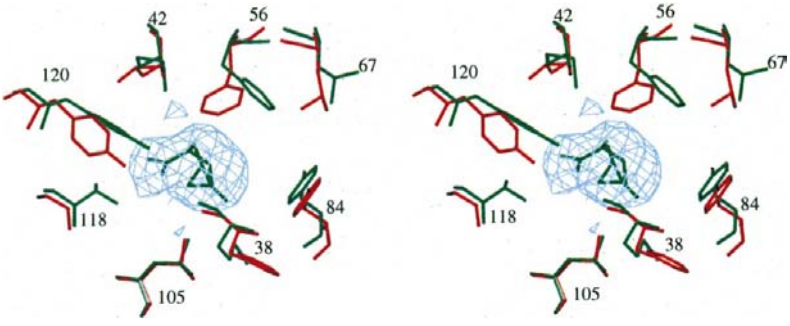

Figure 6
Some of the cavity-lining residues of A2U–DLO (green) and MUP (red). Averaged density of DLO is shown in light blue and the best-fitting DLO model is drawn as a green stick model. Note that Tyr120 points straight towards the ligand density.

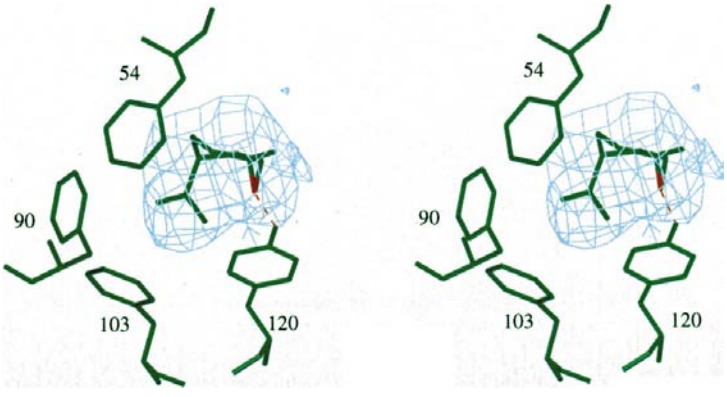

Figure 7
Illustration of the concave wall and Tyr120 in A2U–DLO (green), together with the docked model of *cis* DLO (green; epoxide oxygen in red). Note that the isopropylene moiety is occupying an axial position.

4.2. A2U–DLO complex and hyaline droplet nephropathy

The kidney plays an important role in the catabolism of low molecular weight proteins (Mogielnicki *et al.*, 1971; Maack *et al.*, 1979). Proteins of size 10–90 kDa easily filter through the glomerulus. A major portion of filtered protein is reabsorbed and proteolysed in renal tubular cells. It has been shown that a large portion of the filtered A2U is reabsorbed in the renal tubule of rat (Neuhaus & Lerseth, 1979). However, unlike A2U and RBP, MUP is not reabsorbed in mouse kidney (Lehman-McKeeman & Caudill, 1992*a*). DLO bound to A2U decreases *in vitro* lysosomal degradation by 33% (Lehman-McKeeman *et al.*, 1990). Normal catabolic processing of A2U bound to the xenobiotics is hampered, leading to accumulation and eventually to histologically evident 'hyaline' droplets inside the tubular cells (Borghoff *et al.*, 1990; Lehman-McKeeman, 1993).

The average half-life of a protein in adult male rat liver is about 3 d. There can be various factors contributing to the half-life of a protein such as size, surface charge and hydrophobicity (Beynon & Bond, 1986). The initial event of degradation may or may not involve proteolysis, covalent modification, denaturation or a combination of these.

Proteolytically sensitive sites are the most flexible parts of the protein. There is evidence that ligand binding can stabilize a protein and increase its half-life (Beynon & Bond, 1986).

It has been shown that leupeptin, an inhibitor of cathepsin B, can cause a similar effect as gasoline in male rats (Olson *et al.*, 1988). DLO itself has been shown not to inhibit proteolytic enzymes as such (Lehman-McKeeman *et al.*, 1990). These facts, together with our results, indicate that ligand binding may not bring about any drastic change in the protein to form hyaline droplets, but rather stabilizes the protein by complexing with it which renders it less susceptible to proteolysis inside the lysosome. The estimated half-life of the A2U–DLO complex is ∼50% greater than that of A2U (Lehman-McKeeman *et al.*, 1990). As pointed out by other investigators (Borghoff *et al.*, 1990; Hard & Whysner, 1994), the kinetically controlled accumulation of intact proteins over a longer than average period of time might be a plausible cause of hyaline droplet nephropathy.

The authors wish to thank Drs Derek Ogg and Jonas Uppenberg for their contributions to the early stages of this project, Dr S. E. V. Phillips (Leeds University, England) for providing us with the coordinates of the monoclinic crystal form of A2U and Drs Bill Laidig and Mike Schmidt of the CADMol group of the University of Florida for generating coordinates of plausible conformations of DLO. BNC wishes to thank the tutors at the CCP4 Molecular Replacement workshop held in York (England) in March 1996 for their assistance in solving the structure of the complex of A2U and DLO. This work was supported by Uppsala University and the Swedish Natural Science Research Council. GJK is supported by the Swedish Foundation for Strategic Research and its Structural Biology Network (SBNet).

References

Banaszak, L., Winter, N., Xu, Z., Bernlohr, D. A., Cowan, S. & Jones, T. A. (1994). *Adv. Protein Chem.* **45**, 89–151.

Beynon, R. J. & Bond, J. S. (1986). *Am. J. Physiol.* **251**, C141–C152.

Bianchet, M. A., Bains, G., Pelosi, P., Pevsner, J., Snyder, S. H., Monaco, H. L. & Amzel, L. M. (1996). *Nature Struct. Biol.* **3**, 934–939.

Böcskei, Z., Groom, C. R., Flower, D. R., Wright, C. E., Phillips, S. E. V., Cavaggioni, A., Findlay, J. B. C. & North, A. C. T. (1992). *Nature (London)*, **360**, 186–188.

Bomhard, E., Marsmann, M., Ruhl-Fehlert, C. & Zywietz, A. (1990). *Arch. Toxicol.* **64**, 530–538.

Borghoff, S. J., Miller, A. B., Bowen, J. P. & Swenberg, J. A. (1991). *Toxicol. Appl. Pharmacol.* **107**, 228–238.

Borghoff, S. J., Short, B. G. & Swenberg, J. A. (1990). *Annu. Rev. Pharmacol. Toxicol.* **30**, 349–367.

Brownlow, S., Morais Cabral, J. H., Cooper, R., Flower, D. R., Yewdall, S. J., Polikarpov, I., North, A. C. T. & Sawyer, L. (1997). *Structure*, **5**, 481–495.

Brünger, A. T. (1990*a*). *X-PLOR. A System for Crystallography and NMR.* Yale University, New Haven, Connecticut, USA.

Brünger, A. T. (1990*b*). *Acta Cryst.* A**46**, 46–57.

Brünger, A. T. (1992). *Nature (London)*, **355**, 472–475.

Brünger, A. T., Adams, P. D., Clore, G. M., Delano, W. L., Gros, P., Grosse-Kunstleve, K. W., Jiang, J. S., Kuszewski, J., Nilges, M., Pannu, N. S., Read, R. J., Rice, L. M., Simonson, T. & Warren, G. L. (1998). *Acta Cryst.* D**54**, 905–921.

Brünger, A. T., Krukowski, A. & Erickson, J. W. (1990). *Acta Cryst.* A**46**, 585–593.

Brünger, A. T., Kuriyan, J. & Karplus, M. (1987). *Science*, **235**, 458–460.

Chatterjee, R., Motwani, N. M. & Roy, A. K. (1982). *Biochim. Biophys. Acta*, **698**, 22–28.

Collaborative Computational Project, Number 4 (1994). *Acta Cryst.* D**50**, 760–763.

Cowan, S. W., Newcomer, M. E. & Jones, T. A. (1990). *Proteins Struct. Funct. Genet.* **8**, 44–61.

Cowley, J. J. (1978). *Biological Determinant of Sexual Behaviour*, edited by J. B. Hutchinson, pp. 87–125. Chichester: Wiley.

Dietrich, D. R. & Swenberg, J. A. (1991). *Cancer Res.* **51**, 3512–3521.

Engh, R. A. & Huber, R. (1991). *Acta Cryst.* **47**, 392–400.

Flower, D. R. (1996). *Biochem. J.* **318**, 1–14.

Flower, D. R., North, A. C. T. & Attwood, T. K. (1993). *Protein Sci.* **2**, 753–761.

Hamlin, R., Cork, C., Howard, A., Nielsen, C., Vernon, W., Matthews, D., Xuong, N. H. & Perez-Mendez, V. (1981). *J. Appl. Cryst.* **14**, 85–93.

Hard, G. C. & Whysner, J. (1994). *Crit. Rev. Toxicol.* **24**, 231–254.

Holden, H. M., Rypniewski, W. R., Law, J. H. & Rayment, I. (1987). *EMBO J.* **6**, 1565–1570.

Howard, A. J., Nielsen, C. & Xuong, N. H. (1985). *Methods Enzymol.* **114**, 452–472.

Huber, R., Schneider, M., Epp, O., Mayr, I., Messerschmidt, A., Pflugrath, J. & Kayser, H. (1987). *J. Mol. Biol.* **195**, 423–434.

Jones, T. A. (1992). *Proceedings of the CCP4 Study Weekend. Molecular Replacement*, edited by E. J. Dodson, S. Glover & W. Wolf, pp. 91–105. Warrington: Daresbury Laboratory.

Jones, T. A., Bergfors, T., Sedzik, J. & Unge, T. (1988). *EMBO J.* **7**, 1597–1604.

Jones, T. A., Zou, J. Y., Cowan, S. W. & Kjeldgaard, M. (1991). *Acta Cryst.* A**47**, 110–119.

Kim, S., Qualls, C. W., Reddy, G. & Stair, E. L. (1997). *Toxicol. Pathol.* **25**, 195–201.

Kleywegt, G. J. (1996). *Acta Cryst.* D**52**, 842–857.

Kleywegt, G. J. (1999). *J. Mol. Biol.* **285**, 1887–1897.

Kleywegt, G. J. & Brünger, A. T. (1996). *Structure*, **4**, 897–904.

Kleywegt, G. J. & Jones, T. A. (1994*a*). *Proceedings of the CCP4 Study Weekend. From First Map to Final Model*, edited by S. Bailey, R. Hubbard & D. A. Waller, pp. 59–66. Warrington: Daresbury Laboratory.

Kleywegt, G. J. & Jones, T. A. (1994*b*). *Acta Cryst.* D**50**, 178–185.

Kleywegt, G. J. & Jones, T. A. (1995). *Structure*, **3**, 535–540.

Kleywegt, G. J. & Jones, T. A. (1996*a*). *Structure*, **4**, 1395–1400.

Kleywegt, G. J. & Jones, T. A. (1996*b*). *Acta Cryst.* D**52**, 829–832.

Kleywegt, G. J. & Jones, T. A. (1997*a*). *Methods Enzymol.* **277**, 208–230.

Kleywegt, G. J. & Jones, T. A. (1997*b*). *Methods. Enzymol.* **277**, 525–545.

Kleywegt, G. J. & Jones, T. A. (1998). *Acta Cryst.* D**54**, 1119–1131.

Kristiansen, E. & Madsen, C. (1995). *Toxicol. Lett.* **80**, 147–152.

Laskowski, R. A., MacArthur, M. W., Moss, D. S. & Thornton, J. M. (1993). *J. Appl. Cryst.* **26**, 283–291.

Lee, B. & Richards, F. M. (1971). *J. Mol. Biol*, **55**, 379–400.

Lehman-McKeeman, L. D. (1993). *Toxicology of the Kidney*, edited by J. B. Hook & R. S. Goldstein, pp. 477–494. New York: Raven Press Ltd.

Lehman-McKeeman, L. D. & Caudill, D. (1992*a*). *Toxicol. Appl. Pharmacol.* **112**, 214–221.

Lehman-McKeeman, L. D. & Caudill, D. (1992*b*). *Toxicol. Appl. Pharmacol.* **116**, 170–176.

Lehman-McKeeman, L. D., Caudill, D., Rodriguez, P. R. & Eddy, C. (1998). *Toxicol. Appl. Pharmacol.* **149**, 32–40.
Lehman-McKeeman, L. D., Rivera-Torres, M. I. & Caudill, D. (1990). *Toxicol. Appl. Pharmacol.* **103**, 539–548.
Lehman-McKeeman, L. D., Rodriguez, P. A., Takigiku, R., Caudill, D. & Fey, M. L. (1989). *Toxicol. Appl. Pharmacol.* **99**, 250–259.
Luzzati, V. (1952). *Acta Cryst.* **5**, 802–810.
Maack, T., Johnson, V., Kau, S. T., Figueiredo, J. & Sigulem, D. (1979). *Kidney Int.* **16**, 251–270.
McPherson, A. J. (1982). *Preparation and Analysis of Protein Crystals.* New York: John Wiley and Sons.
Matthews, B. W. (1968). *J. Mol. Biol.* **33**, 491–497.
Mogielnicki, R. P., Waldmann, T. A. & Strober, W. (1971). *J. Clin. Invest.* **50**, 901–901.
Monaco, H. L., Zanotti, G., Spadon, P., Bolognesi, M., Sawyer, L. & Eliopoulos, E. E. (1987). *J. Mol. Biol.* **197**, 695–706.
Navaza, J. (1994). *Acta Cryst.* A**50**, 157–163.
Navaza, J. & Saludjian, P. (1997). *Methods Enzymol.* **276**, 581–594.
Neuhaus, O. W. & Lerseth, D. S. (1979). *Kidney Int.* **16**, 409–415.
Newcomer, M. E. (1993). *Structure*, **1**, 7–18.
Newcomer, M. E., Jones, T. A., Åqvist, J., Sundelin, J., Eriksson, U., Rask, L. & Peterson, P. A. (1984). *EMBO J.* **3**, 1451–1454.
Olson, M. J., Mancini, M. A., Garg, B. D. & Roy, A. K. (1988). *Toxicol. Lett.* **41**, 245–254.
Otwinowski, Z. & Minor, W. (1997). *Methods Enzymol.* **276**, 307–326.
Papiz, M. Z., Sawyer, L., Eliopoulos, E. E., North, A. C. T., Findlay, J. B. C., Sivaprasadarao, R., Jones, T. A., Newcomer, M. E. & Kraulis, P. J. (1986). *Nature (London)*, **324**, 383–385.
Pervaiz, S. & Brew, K. (1985). *Science*, **228**, 335–337.
Ramakrishnan, C. & Ramachandran, G. N. (1965). *Biophys. J.* **5**, 909–933.
Ridder, G. M., Von Bargen, E. C., Alden, C. L. & Parker, R. D. (1990). *Fundam. Appl. Toxicol.* **15**, 732–743.
Rossmann, M. G. (1972). Editor. *The Molecular Replacement Method. A Collection of Papers on the Use of Non-Crystallographic Symmetry.* New York: Gordon and Breach.
Rossmann, M. G. & Blow, D. M. (1962). *Acta Cryst.* **15**, 24–31.
Roy, A. K., Neuhaus, O. W. & Harmison, H. R. (1966). *Biochim. Biophys. Acta*, **127**, 72–81.
Stonard, M. D., Phillips, P. G., Foster, J. R., Simpson, M. G. & Lock, E. A. (1986). *Clin. Chim. Acta*, **160**, 197–203.
Takahashi, K., Lindamood, C. & Maronpot, R. R. (1993). *Environ. Health Perspect.* **101**, 281–285.
Tegoni, M., Ramoni, R., Bignetti, E., Spinelli, S. & Cambillau, C. (1996). *Nature Struct. Biol.* **3**, 863–867.
Toh, H., Kubodera, H., Nakajima, N., Sekiya, T., Eguchi, N., Tanaka, T., Urade, Y. & Hayashi, O. (1996). *Protein Eng.* **9**, 1067–1082.
Vriend, G. & Sander, C. (1993). *J. Appl. Cryst.* **26**, 47–60.
Zanotti, G., Marcello, M., Malpeli, G., Folli, C., Sartori, G. & Berni, R. (1994). *J. Biol. Chem.* **269**, 29613–29620.
Zanotti, G., Ottonello, S., Berni, R. & Monaco, H. L. (1993). *J. Mol. Biol.* **230**, 613–624.